

PARAMETRIC X-RAY DETECTION IN UA9 EXPERIMENT

Dabagov S.B.^{1,2,3}, Capitolo E.¹, Gogolev A.⁴, Hampai D.¹, Liedl A.¹, Polese C.¹

Participant Institutions:

¹ INFN - LNF, XLab Frascati - Via E. Fermi, 40, I-00044 Frascati (Rome), Italy

² P.N. Lebedev Physical Institute, Moscow

³ National Research Nuclear University "MEPhI", Moscow

⁴ Tomsk Polytechnic University, Lenin Avenue 30, Tomsk 634050, Russia

Parametric X-Ray radiation (PXR) is a phenomenon due to the interaction of charged particles inside a crystal well ordered lattice. The passage of the particles inside the potential field into the crystal causes small deflections which result in radiation emissions. By this way the emission is diffracted by the crystal planes. In this work the results of the last five years of activity on PXR detection during UA9 experiment are reported. The beam provided in H8 area, protons or Pb ions, is channeled inside different crystals and PXR emission is detected.

1 First attempt

The first attempt to observe PXR radiation at UA9 experiment is dated in 2010. For this experimental run a beam composed by 400 GeV/c protons, with measured RMS divergence $\sigma_x=10.7 \mu\text{rad}$ and $\sigma_y=7.6 \mu\text{rad}$, was provided. The average cycle time was 45s with a pulse duration of 10s and an average of $(1.3\pm 0.1)\cdot 10^6$ particles per spill. The beam is analyzed through different microstrip detectors represented, with labels S, in Fig. 1.

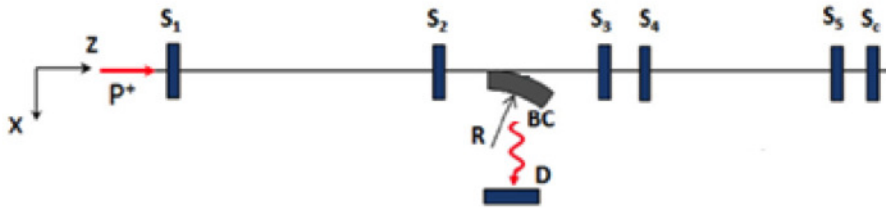


Figure 1: PXR Scheme. The microstrip detectors are labeled by S. The bent crystal, BC, is struck by the proton beam, p, and the PXR signal is detected by detector, D.

In this first attempt the detector used for the observation was a semiconductor silicon detector with a 13 mm^2 active area and a $25 \mu\text{m}$ beryllium window. The distance crystal-detector was in the range $[94,127] \text{ mm}$ and a cylindrical collimator (diameter 5 mm, length 50 mm) was placed between them. The entire detection system was placed inside a lead cavity in order to reduce the radiation noise. During the experiment three crystals were analyzed: one quasi-mosaic (QM) crystal and two strip (ST) crystal. The beam was parallel to the deflecting planes, (111) for QM crystal and (110) for ST. An high precision goniometer allowed the orientation of the crystal with an accuracy of $2 \mu\text{rad}$. QM crystal was $40\times 30\times 2 \text{ mm}^3$ (Height x Width x Thickness) while ST1 $70\times 5\times 2 \text{ mm}^3$ and ST2 $70\times 5\times 0.4 \text{ mm}^3$.

Reflection Order	QM	ST
1 st	5.58 keV	6.46 keV
2 nd	11.18 keV	12.85 keV
3 rd	16.70 keV	19.31 keV

Table 1: PXR characteristic emission for QM and ST crystals.

Reflection order	PXR signal [counts]	Flux [phot/prot 10 ⁻⁷]	Acquisition time [hour]
QM			
1 st	420±20	6.9±0.8	7.8
2 nd	230±16	3.8±0.4	
3 rd	47±8	0.77±0.12	
ST1			
1 st	179±13	3.4±0.4	6.75
2 nd	101±10	1.9±0.3	
ST2			
1 st	287±17		
2 nd	62		

Table 2: Results for the observation of PXR signal for QM and ST crystals.

The PXR characteristic emission lines energies for these crystals are summarized in Tab. 1.

Due to the low emission of the PXR signal the observation has a duration of several hours. In the Tab. 2 the results are summarized.

The spectra acquired during this observation are shown in Fig. 2. By looking at these spectra it is possible to realize that QM crystal has greater emission due to the higher density of the reflecting planes (110). Furthermore, when comparing the two strip crystals the ST2 shows higher intensity than the ST1 probably due to the smaller thickness and consequently the signal is less reduced by the absorption of the radiation within the crystal itself. However, for the ST2 crystal, the proton flux and the acquisition time were not available (not recorded).

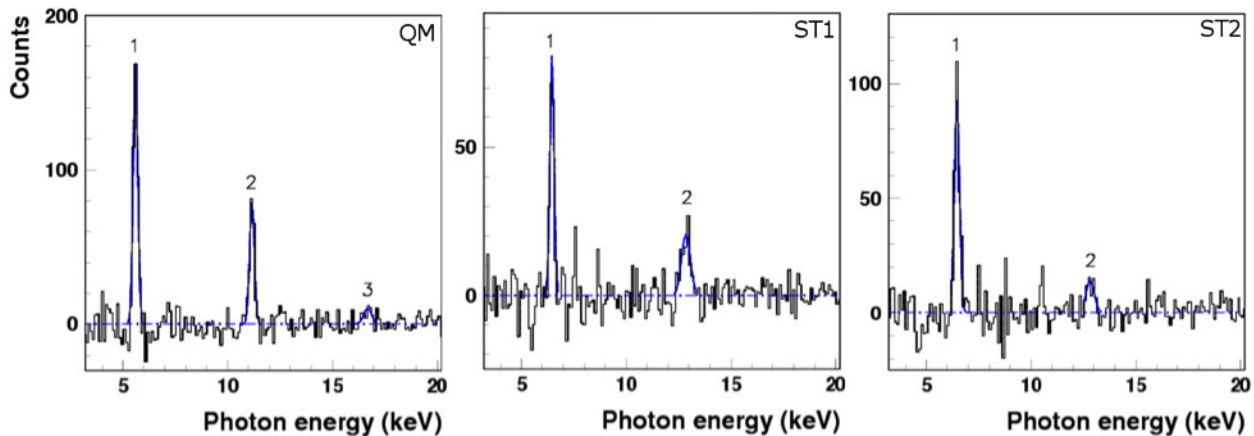


Figure 2: PXR spectra for QM and ST crystal. In these spectra the background has been subtracted.

2 Parametric X-ray radiation from Pb Ion Beam: estimations

In this simulation the layout of the numerical experiment is similar to the first attempt [W. Scandale et al., Phys. Lett. B 701 (2011) p. 180]. Fig. 3 shows the layout in the horizontal plane for the experiments with quasi-mosaic (QM) and strip (ST) silicon crystals. A beam of Pb nuclei with energy 158 GeV/u entered a crystal in the collimation geometry being parallel to the deflecting planes, which are the (111) and (110) crystallographic planes for the QM and ST crystals, respectively.

The simulation was carried out for a Gaussian incident beam with the cross-section $\sigma = 1.0 \times 0.7 \text{ mm}^2$ and divergence $\sigma = 10.7 \times 7.8 \text{ } \mu\text{rad}^2$. A beam of Pb ions crosses the crystal with an offset of 0.7 mm depth in the QM case and in the centre in the ST case.

PXR is generated by the particle field crossing a set of the crystallographic planes. PXR reflexes (110) and (100) in the case of (a) and (b) shown in Fig. 3, respectively, was calculated.

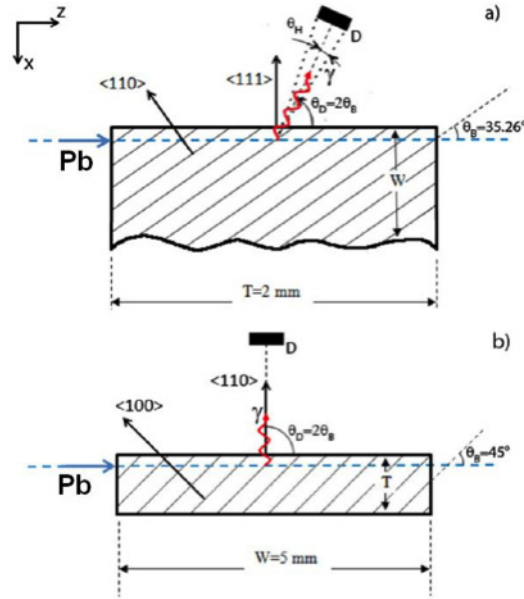


Figure 3: The simulation scheme details: (a) quasi-mosaic crystal, (b) strip crystal.

The energy of PXR photons is determined by the following equation:

$$E_n = n \frac{2\pi\hbar c}{d} \frac{\beta \sin\theta_B}{1 - \beta\sqrt{\varepsilon}\cos\theta_D\cos\theta_y} \quad (1)$$

where n is the diffraction order, d is the interplanar distance, $\beta = v/c$ and ε is the dielectric constant of the target material ($\varepsilon = 1 - (\omega_p/\omega)^2 \approx 1$, ω is the frequency of PXR photons, ω_p is the plasmon frequency), θ_B is the Bragg angle, θ_D and θ_y are the radiation registration angles. θ_D is the angle between the projection of the radiation direction and the momentum in the diffraction plane. θ_y is the angle between projection of the radiation direction on the diffraction plane and the radiation direction. The diffraction plane (shown in Fig. 3) is determined by the particle momentum and by the vector normal to the crystal planes.

According to the formula, PXR photons energy from plane (110) for detection angle ($\theta_D = 2\theta_B$) 70.52° is equal to 5.59 keV and from (100) for detection angle 90° is equal to 6.46 keV. The distance between the crystal and the screen D was 117 and 200 mm for QM and ST crystals, correspondently.

The calculations of PXR parameters have been performed according to the PXR kinematic theory [H. Nitta, Phys. Rev. B 45 (1992) p. 7621], which well describes many experimental results. In the simulation a crystal considered as a set of straight samples and PXR yield from all crystal can be represented as superposition of separate contributions from each sample. It should be noted that, in ideal case, the PXR intensity must increase with the charge number Z of the particle as Z^2 therefore the PXR intensity from nuclei is much more intense than from protons. The dependence on the particle charge was experimentally observed in [Yu.N. Adishchev et al., JETP Lett. 81 (2005) p. 241] with a large error. However, here we have to underline that theoretical prediction for Z^2 -dependence has to be correct for real experimental conditions. Fig. 4 presents the simulation results for the ideal case.

In calculations absorption in the crystal and the air, without convolution detector characteristics (ideal case), were taken into account. Expected values of the intensities are given in Tab. 3.

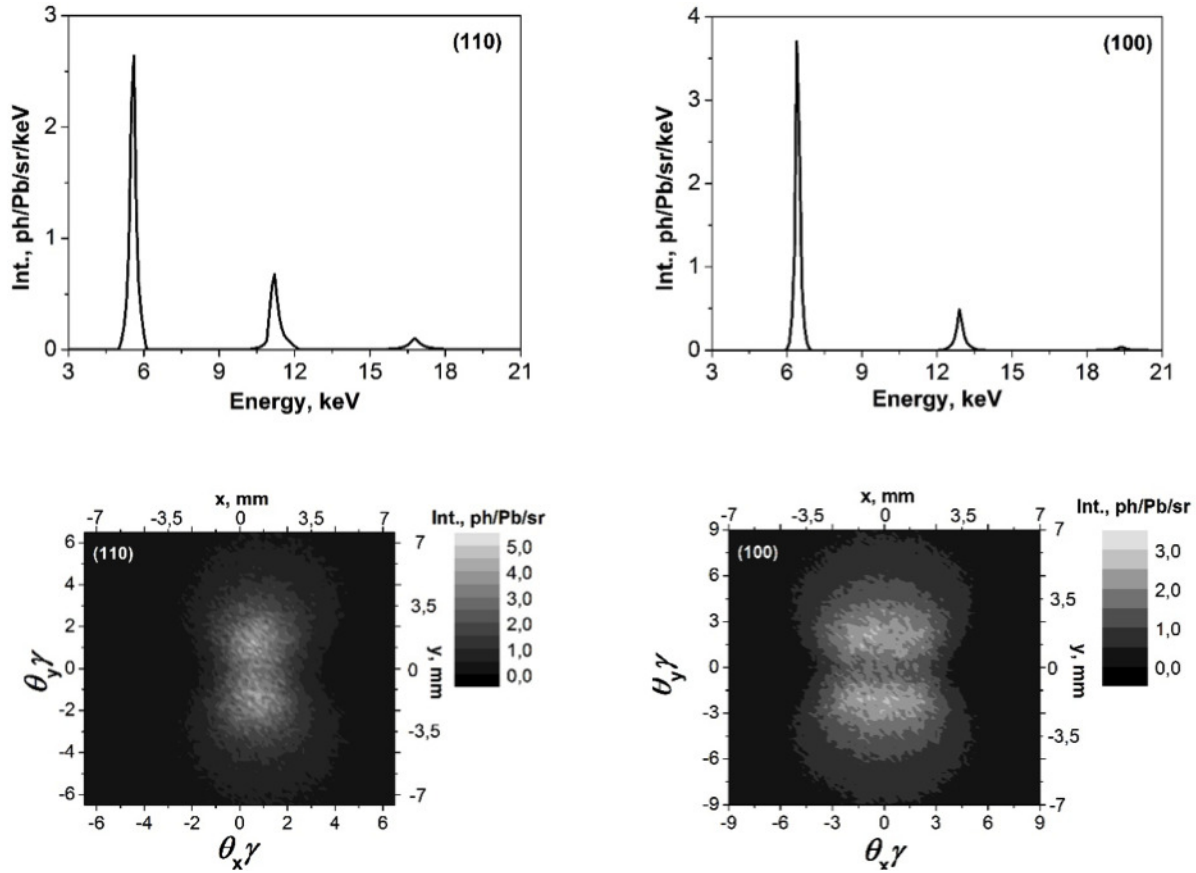


Figure 4: The spectra and angular distributions on the detector plane PXR from QM crystal (left) and ST crystal (right).

Any mistake in the vertical direction-independent positioning of the detector in 1 mm in case of (100) will result in 60% difference between measured and simulated values (the same conclusion is valid also for the (110) orientation).

Reflex	Energy of maximum, (keV)	Intensity I, (ph/Pb/sr)	FWHM, (eV)
(220)	5.6	0.864	258
(440)	11.2	0.314	366
(660)	16.8	0.071	499
(400)	6.4	0.906	211
(600)	12.9	0.179	281
(800)	19.4	0.020	370

Table 3: Simulation results.

3 Observation on 2011

In 2011 the preliminary study by UA9-LNF section in parasitic acquisition was performed. We used a SDD detector by XGLab s.r.l. with a polymeric window (AP3.7) by MoxTek. The run was performed with completely stripped Pb ions characterized by momentum GeV/c and a flux of $2 \cdot 10^4$ charges/spill. The beam size observed was 5.96×5.97 mm.

According on the crystal plane (Si100), the detector was placed at 90° respect to the primary beam, at a distance of 100 mm.

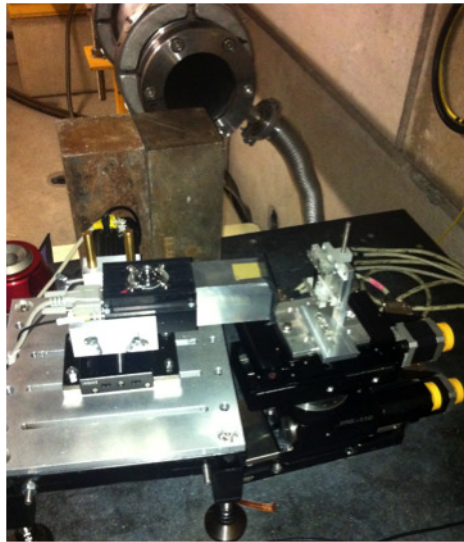


Figure 5: Experimental Layout run 2011. On Gonio it is visible the ST crystal, on the left the SDD detector and the two concrete bricks.

The SDD detector has an active area of 30 mm^2 with an energy resolution of 123 eV at $\text{MnK}\alpha$ and a degradation of energetic resolution of 4 eV at 100 kcps. In order to reduce the noise coming from the primary beam, in particular to expose directly the detector to the pipe window, the SDD was protected by two concrete bricks.

Even if we are not sure of the primary beam spectrum, we had a clear evidence of the PXR emissions. The acquisition time was estimated in 40 hours: such a long acquisition time coupled with a very weak acquisition indicating that the system was not well aligned the beam did not consist of Pb ions only.

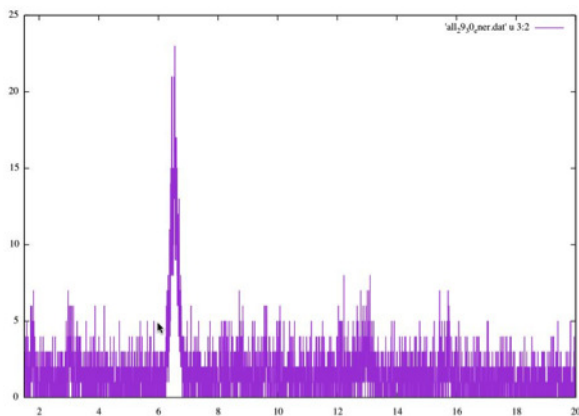


Figure 6: This spectrum is obtained by the sum of two days acquisitions. At 6.5 keV is evident the PXR first order signal and at 13 keV the second order.

XGL-SPCM-4110-CUBE based on 25mm ² SDD:
25 mm ² SDD active area
Beryllium window, thickness 12.5 μ m
Silicon thickness 500 μ m
Case: 47mm finger length, diameter 18mm
Resolution <135eV at MnK α

Table 4: XGLab SDD specifications.

4 Observation on June 2015

The run at H8 of June 2015 was planned for a 400 GeV/c proton beam and the main goal for the PXR acquisition was the testing of a new Silicon Drift Detector. The device in analysis was a XGLab detector with specifications described in Tab. 4.

The detector has been mounted on a linear stage remotely controlled allowing a movement parallel to the beam in a range of 100 mm, and on a manual vertical movimentation system for the displacement also on this direction.

This time some tracker planes have been added for the analysis of the beam upstream and downstream relative to the crystal such as represented in Fig. 7. The system has been tested in two configurations:

	1 st configuration	2 nd configuration
Collimation	Aluminium :Length 33 mm, Thickness 10 mm, Window diameter 23 mm	No
Shielding	Aluminium: 10 mm	Aluminium: 5 mm Lead: 2 mm
Crystal-Detector Distance	140 mm	30 mm

During this run the acquisition times were between 30 minutes and 1 hour. The detector was put in the supposed best position for the PXR detection.

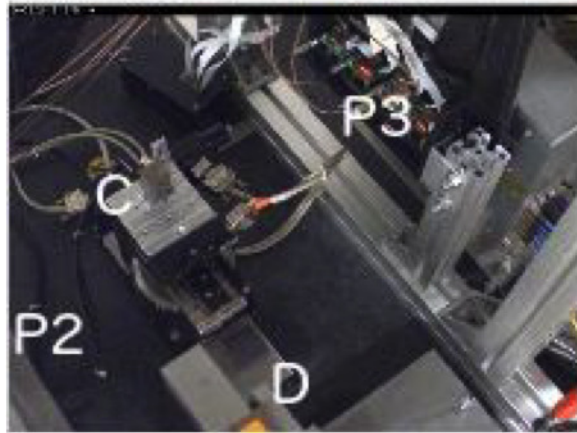


Figure 7: Experimental layout for June 2015. P2 and P3 tracker planes enclose the experimental table. The crystal, C, stricken by the beam emitting PXR signal is analyzed by SDD detector, D.

The beam flux was detected as $2 \cdot 10^6$ particles per spill and results of these acquisitions show how the addition of trackers planes is connected to an increment of two kind of noisy artifacts during the measurement, one in the first interval of energy channels and the other in the last part.

The two spectra in Fig. 8 show how the configuration 2 was less afflicted by the second noise effect, and even that the smaller distance allowed the detection of Si emission from the crystal.

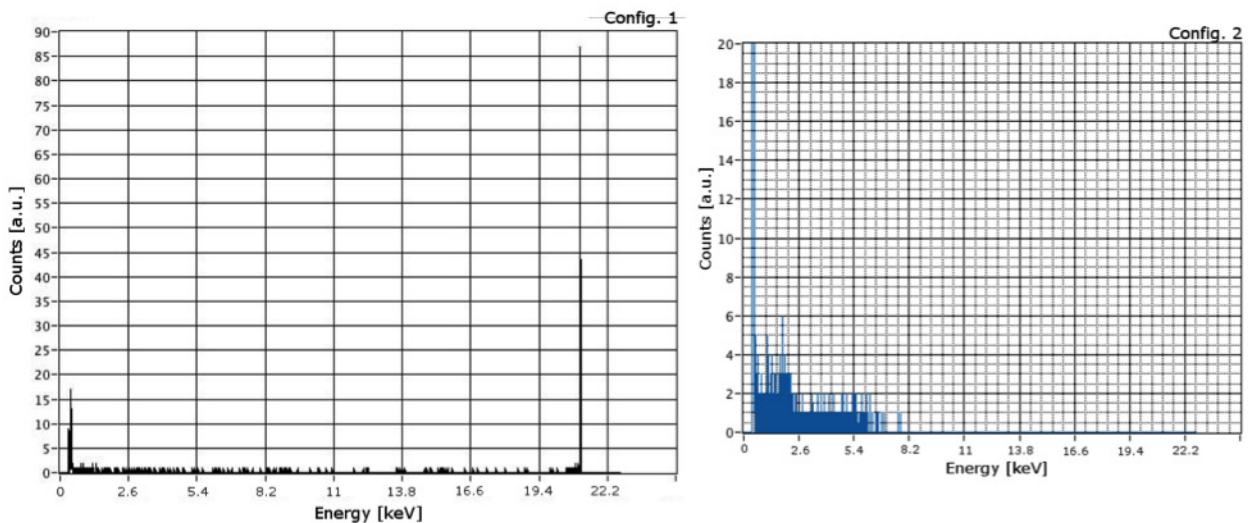


Figure 8: Spectra for the two configuration.

These kind of noise are probably the result of the interpretation of the shape of the signal registered by the detector. The high flux of heterogeneous particles during the 10s spill is wrongly interpreted and generates at high channels a pile-up behavior and in the low channels a sort of bin effect for all the not interpreted signals.

These results brought to some conclusion for the next run:

- Collimation has to be redesigned with the aim of reducing the crystal-detector distance and

observed area

- New shielding system is needed in order to reduce the noise effect coming from the environment, tracker planes in primis
- Movimentation system allowing remotely displacements on the two axis of the plane parallel to the crystal is crucial for the searching of the PXR emission before the long statistics acquiring.

5 Observation on November 2015

For this run a new PXR detection system has been designed.

This device is composed by a two axis movimentation system and the detector placed inside a shielding box. From design to realization, all the process has been curated at INFN-LNF and it is shown in Fig. 9.

The core of the new system is the shielding box designed to guarantee a layer of 2 mm of Pb and more than 6 mm of Al alloy all around the detector (Fig. 10).

The detector finger, with the sensible area, is shielded by the same lead thickness and by a brass probe coupled with a cap of the same material. This cap permits the addition of an internal lead pin-hole.

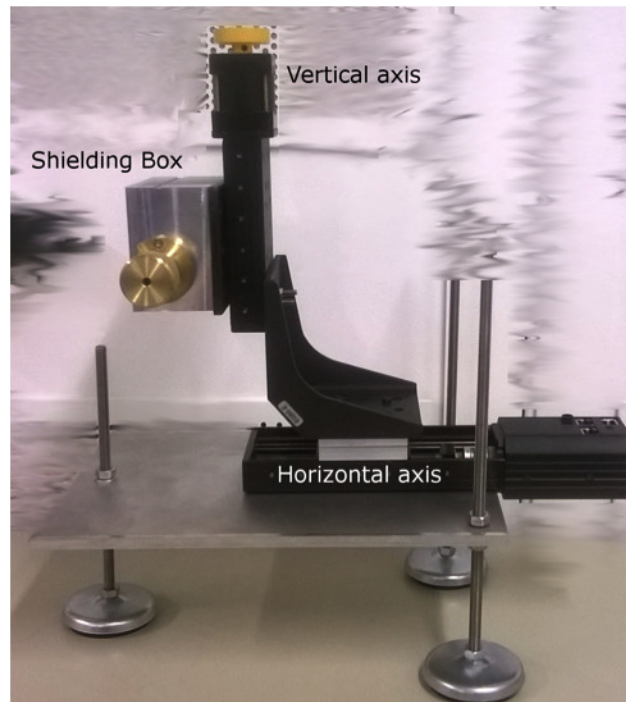


Figure 9: New PXR system. Two linear stages permit scanning parallel to the crystal plane, shielding box covers the detector from the background radiation and allows a first raw alignment.

Last feature of the box are the two lateral grooves. These are suitable to take advantage of the laser system used for the first alignment of the crystal. In this way the detector window can be placed at a distance of 100 mm with a good approximation perpendicular to the beam and on the 75° line from the striking point on the crystal.

At the distance of 100 mm the PXR spot emitted for QM is simulated to be 1×2.5 mm (divergence of 10×25 mrad). Considering a circular active area with diameter of 5.6 mm, a couple

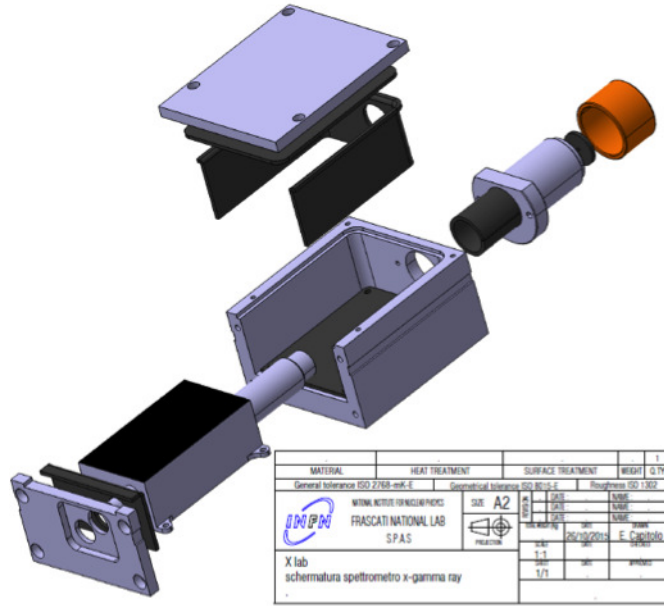


Figure 10: Shielding box exploded view drawing.

Channel	Energy [keV]	Emission Line	Coming from
570	3.006	Ar $K\alpha$	Air
843	4.539	Ti $K\alpha$	Crystal Holder (Ti alloy)
920	4.971	Ti $K\beta$	Crystal Holder (Ti alloy)
1468	8.049	Cu $K\alpha$	Cap of shielding box (brass)
1575	8.650	Zn $K\alpha$	Cap of shielding box (brass)

Table 5: Interpretation of the acquired spectrum.

of mm of misalignment become relevant and a preceding scanning step, before acquisition, for a fine alignment is required.

For these run a Pb Ion beam had been provided. Due to the lack of information about the exact composition of the beam it is not possible to deduce a reliable quantitative analysis of the results. Theoretically a completely stripped Pb ion beam has been provided with a $5 \cdot 10^5$ charges/s flux, the estimated size is on x axis 10 mm, 80 μ rad divergent, and on y 7mm, 100 μ rad divergent.

The crystal in analysis is a Quasi Mosaic, QM46, and due to the large beam size the entire crystal is put in front of it.

The limited available acquisition time has also reduced the chances of the experiment to a single 4 hour acquisition, avoiding also the scanning for the fine alignment. In order to have the maximum active area available, no pin-hole has been applied in front of detector window. However in this way the acceptance angle is opened to any possible scattering and fluorescent signal coming from the crystal area. The acquired spectrum is shown in Fig. 11.

After calibration it is possible to summarize in Table 5 the results.

The spectrum points out that the alignment was not enough precise. In optimal condition the detector should be rotated in 15° respect to the real position used. In that case it would be possible to collect all the PXR cone, while during our measurements the half part of the working

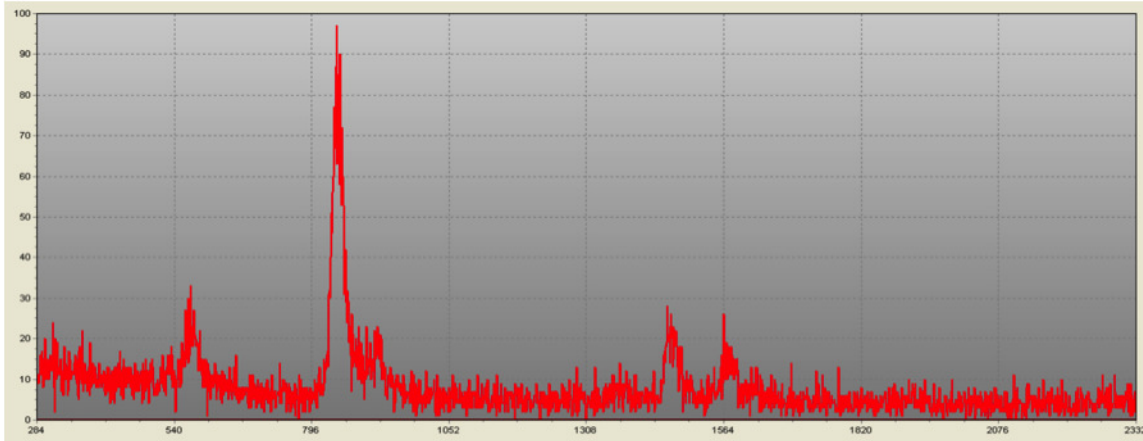


Figure 11: Spectrum acquired for 4h. Five peaks are clearly visible.

windows was shadowed by the brass shielding cap.

As we can conclude, the detected radiation is due to the fluorescence of air (Ar), crystal holder (Ti alloy) and the cap of shielding box (brass). This hypothesis is confirmed by the comparable intensities of the peaks of channels 1468 and 1575 relative to Cu and Zn, as the specific brass used for the shielding is the CuZn40Pb2 alloy (Cu \approx 60% and Zn \approx 40%). The fluorescence of Si is absorbed by the air path between crystal and detector.

6 Conclusion

In 2011, having a 40h run duration, the evidence of PXR emission by the Pb ion beam was clear but the lack of information on the primary beam composition avoided the possibility of any detailed analysis.

In November 2015 while the run duration was approximately one order less, 4h, assuming that we have even detected PXR, our estimation proves that the low flux of radiation was not enough to be resolved for this S/N ratio in presence of other fluorescence contribution, even for primary emission, integral less than 20. The problem can be solved in the same experimental conditions just by increasing the recording time (dedicated for the PXR) up to 8-10 hours.

Another important point is that the quality of the primary ion beam must be well defined: all our estimation have been done supposing complete stripped Pb ions beam, information not confirmed by the machine group.

We also know that the transverse size of the beam exceeds the front cross section of crystal reducing the number of particles emitting PXR by almost one order of magnitude. On the other hand the part of beam out of crystal front entrance contributes to the fluorescence of the Titanium Crystal holder, clearly detected.

7 Future aims

In the next run it will be required:

- Enough time for the detection of the signal: either dedicated or parasitic without changes.
- A scanning procedure for the searching of the best alignment position.
- With the best alignment, also the application of a pinhole for the increase of the S/N of the entire measurement.

- The description of the beam composition in order to compare theoretical hypothesis and experimental observation
- Such first attempt ST crystals are preferred for the easier alignment procedure: the 90° emission is more easily detectable.